Flux Ropes Are Born in Pairs: An Outcome of Interlinked, Reconnecting Flux Tubes

Christopher T. Russell[1] and Yi Qi[2]

[1]University of California Los Angeles
[2]Unknown

November 24, 2022

Abstract

Flux transfer events are transient magnetized plasma structures that are self-balancing, rope-like phenomena that can appear at the Earth's magnetopause when the interplanetary magnetic field is southward. The formation of this type of flux rope has been unclear. Using measurements of particles and magnetic fields on the MMS spacecraft, we find that rope-like structures containing magnetospheric energetic electrons have exactly the same occurrence rate as those without magnetospheric electrons, independent of solar wind properties and location of observation. This equality is consistent with a pair of flux ropes being generated at the same time as an outcome of magnetic flux pileup reconnection. One resulting flux rope has its two ends connected to the magnetosphere, and the other is connected on both ends to the shocked solar wind.

Flux Ropes Are Born in Pairs: An Outcome of Interlinked, Reconnecting Flux Tubes

C.T. Russell[1], Yi Qi[1]

[1]Earth Planetary and Space Sciences, University of California, Los Angeles, CA 90095-1567, USA.

Corresponding author: C.T. Russell (ctrussell@igpp.ucla.edu)

Key Points:

- An inventory of twisted self-balancing flux ropes at the Earth's magnetopause indicates they are produced in pairs.
- The extent of the magnetopause simultaneously undergoing reconnection leads to entangled magnetic flux pulling in opposite directions.
- Where flux tubes pull against each other becomes a site of reconnection, producing one flux tube doubly connected, and one disconnected.

Abstract

Flux transfer events are transient magnetized plasma structures that are self-balancing, rope-like phenomena that can appear at the Earth's magnetopause when the interplanetary magnetic field is southward. The formation of this type of flux rope has been unclear. Using measurements of particles and magnetic fields on the MMS spacecraft, we find that rope-like structures containing magnetospheric energetic electrons have exactly the same occurrence rate as those without magnetospheric electrons, independent of solar wind properties and location of observation. This equality is consistent with a pair of flux ropes being generated at the same time as an outcome of magnetic flux pileup reconnection. One resulting flux rope has its two ends connected to the magnetosphere, and the other is connected on both ends to the shocked solar wind.

Plain Language Summary

The Earth's intrinsic magnetic field deflects the solar wind flow at a boundary called the magnetopause. Near this boundary, twisted flux tubes are found when the external field in the solar wind is nearly oppositely directed to that of the Earth. These tubes are found to be of two types: devoid of and containing energetic electrons. Under all conditions, there are equal numbers of these two types of magnetic structures. This paper suggests a possible mechanism of how these pairs of structures can be generated and an updated understanding of how this will influence the magnetic flux transfer between the solar wind and the earth's magnetosphere.

1 Introduction

In 1977, the dual spacecraft International Sun-Earth Explorer mission was launched into a single, high-apogee orbit with a variable separation between the two spacecraft. One of its first discoveries was that near the Earth's magnetopause, there were detached (in the time domain) flux ropes (FRs). These flux ropes often contained energetic electrons, signaling that they might be connected to the Earth's magnetosphere and its plasma sheet (Russell and Elphic, 1978). For example, Figure 1 shows the time series of the magnetic field at ISEE 1 and 2, for over an hour on November 8, 1977. At 0212 UT and 0236 UT, the spacecraft entered a strong field region similar in strength to that of the magnetic field in the magnetosphere after 0250 UT, but these fields had a quite different orientation. This transient feature was termed as a flux transfer event (FTE) by the authors. It was postulated to be evidence of a flux rope that had become connected between the magnetosheath and the magnetosphere, convected away from the subsolar region and supposedly transferring that flux inventory of the magnetotail. These flux ropes are macroscopic structures containing up to about 20 M Webers magnetic flux, but flux ropes of much smaller size are also found in the higher resolution MMS data (Russell et al., 2017).

Lee and Fu (1985) proposed a different model: ropes formed by the occurrence of multiple X lines. However, the ropes shown in the time series of Figure 1 appear to be well detached from the magnetosphere and not simply part of the magnetopause, as they would be in this latter model. The launch of the 4-spacecraft MMS mission has enabled the identification of many such flux ropes near the magnetopause. All of the "flux transfer events" found with the MMS mission were consistent with self-balancing magnetic ropes (Zhao, 2019). Any successful FTE model must simultaneously explain the self-balancing flux-rope nature of the FTE, as well as the apparent detachment of the twisted flux tube from the magnetopause.

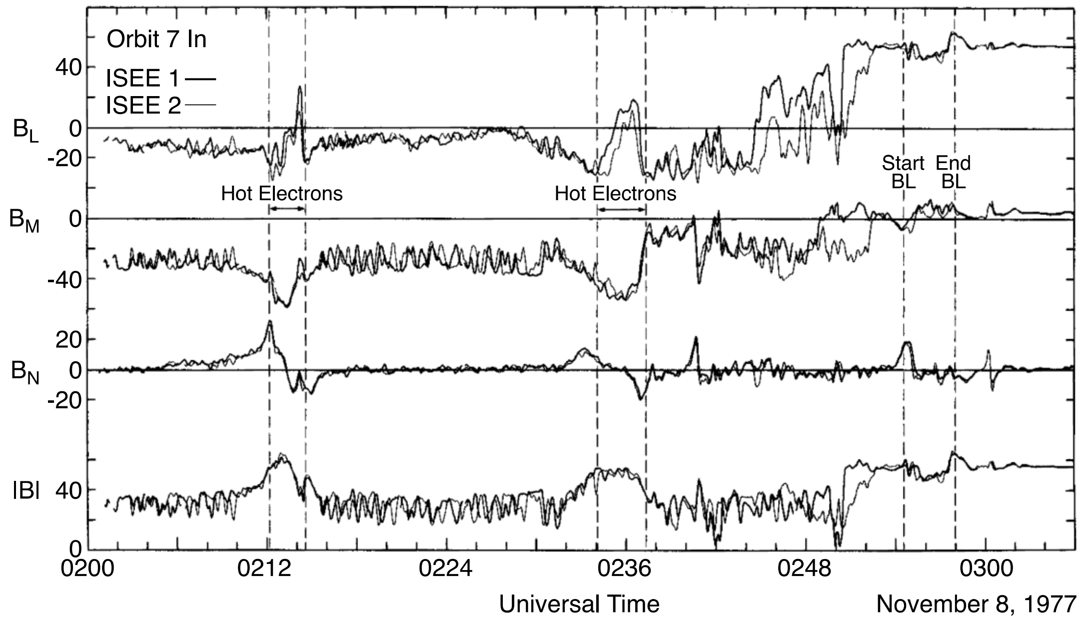

Figure 1. The time series of the magnetic field measurements by ISEE-1 that showed the magnetic field and energetic electrons at the Earth magnetopause, indicating that the magnetic flux ropes were formed at the magnetopause when the interplanetary field was southward and that these ropes could carry energetic magnetospheric electrons. (Russell and Elphic, 1979)

2 Flux Rope Properties

Figure 2a shows an idealized sketch of a self-balancing magnetic rope. The twisted magnetic field applies an inward tension force balanced by the outward total pressure gradient force. We attribute such twisting to the shear in the flow near the magnetopause. Such structures are seen near the magnetopause and have been studied by many authors between their initial discovery and the launch of MMS (Burch et al., 2016). The MMS plasma spectrometer (Pollock et al., 2016) and magnetometer (Russell et al., 2014) allow the structure of these ropes to be studied in detail. In the MMS data, flux ropes clearly are of two types: one populated with electron flux of magnetospheric energies (Type A), and the other without such electron flux (Type B). Figure 2b, c shows examples of these two different types of flux ropes with time series of the magnetic field, as well as the energetic ion and electron flux. Energetic electrons are clearly seen in Figure 2b, but not in Figure 2c.

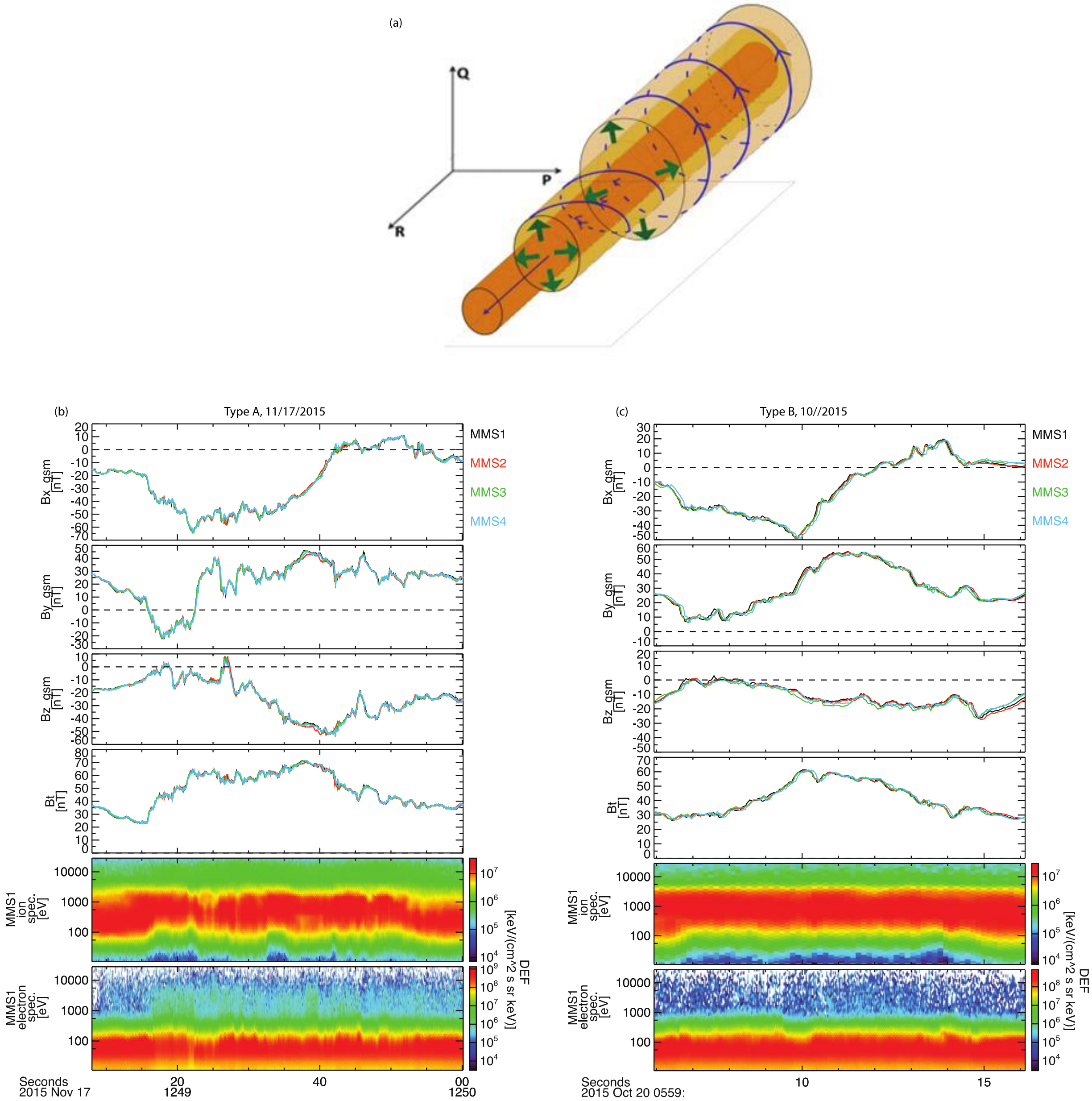

Figure 2. (a) Sketch of the internal structure of a magnetic flux rope, whose magnetic and plasma pressure forces combine to create an equilibrium of forces. Curvature force presses inward, and pressure gradient force presses outward; purple lines surrounding the rope represent the magnetic field lines; green arrows indicate the magnetic pressure. The rope coordinate system is defined as follows: R points to the rope axial direction along which the pressure gradient is minimum; Q is defined by the transverse crossing, the direction is obtained by four-spacecraft timing; P completes the right-hand coordinates; **(b), (c)**: Time series of magnetic field and plasma and particle data during two intervals. During the first interval, energetic electrons are present (Type A), but in the second interval, they are not (Type B). This indicates that the first flux rope is connected to the magnetosphere with trapped electrons inside, and during the

second interval, the flux rope does not contain any electrons and thus seems not to connect with the radiation belts.

3 Two types of Flux Ropes: Statistical study

Do the A and B events have any differences besides the presence or absence of energetic electrons? One possible difference could be that two classes of events occur in different regions along the magnetopause. We examine this possibility in Figure 3. During MMS mission phase 1a, 98 flux ropes were observed, and 47 of them were identified as type A (plus) while the rest 51 were type B (triangle). Their spatial distributions are shown in the GSM Y-X plane in panel a, in the Z-X plane in panel b, and in the Z-Y plane in panel c of Figure 3. There seems to be no difference in the spatial distributions of the two classes. The ropes with magnetospheric particles are definitely on closed trapping field lines, since any open field lines would be rapidly nearly empty of energetic particles. However, there is no clear difference in the spatial distribution of empty and filled flux ropes. Half the tubes have energetic electrons and half do not, regardless of where our samples are obtained.

The magnetic field strength also appears to be the same. The peak-to-peak magnetic field is the same as the peak-to-peak magnetic field divided by the core field strength, as shown in Figure 3d, e. When the total flux content of the two types of flux ropes is calculated, their flux contents are indistinguishable, as shown in Figure 3f.

The occurrence rate of these two types of flux ropes also seems independent of the type. Figure 3g shows the distribution of the IMF B_Z GSM magnetic field strength in 2 nT bins. The occurrence rate peaks around 0 nT and becomes almost zero at ±10 nT. We use this distribution to normalize the occurrence rate of FRs as a function of IMF B_Z values, which we show in Figure 3h. For northward positive B_Z, there are a few flux ropes, but not many. The rate increases for increasingly southward IMF B_Z (as normalized by the IMF B_Z occurrence) until the (-6 to -4nT) bin, when the rate suddenly drops. We have only one event at this large-negative-B_Z-value bin, implying a dramatically decreasing occurrence rate, considering the gradually decreasing IMF distribution under this extreme circumstance. This behavior is possibly not a statistical fluke, but rather signals that rope production does not occur for large magnetic B_Z of about -10 nT and stronger. Again, there is no discernible difference between the ropes that have magnetospheric electron fluxes, and those that do not. There is no statistically significant dependence of the rate of flux rope production or difference between A and B rates (Zhao, 2019).

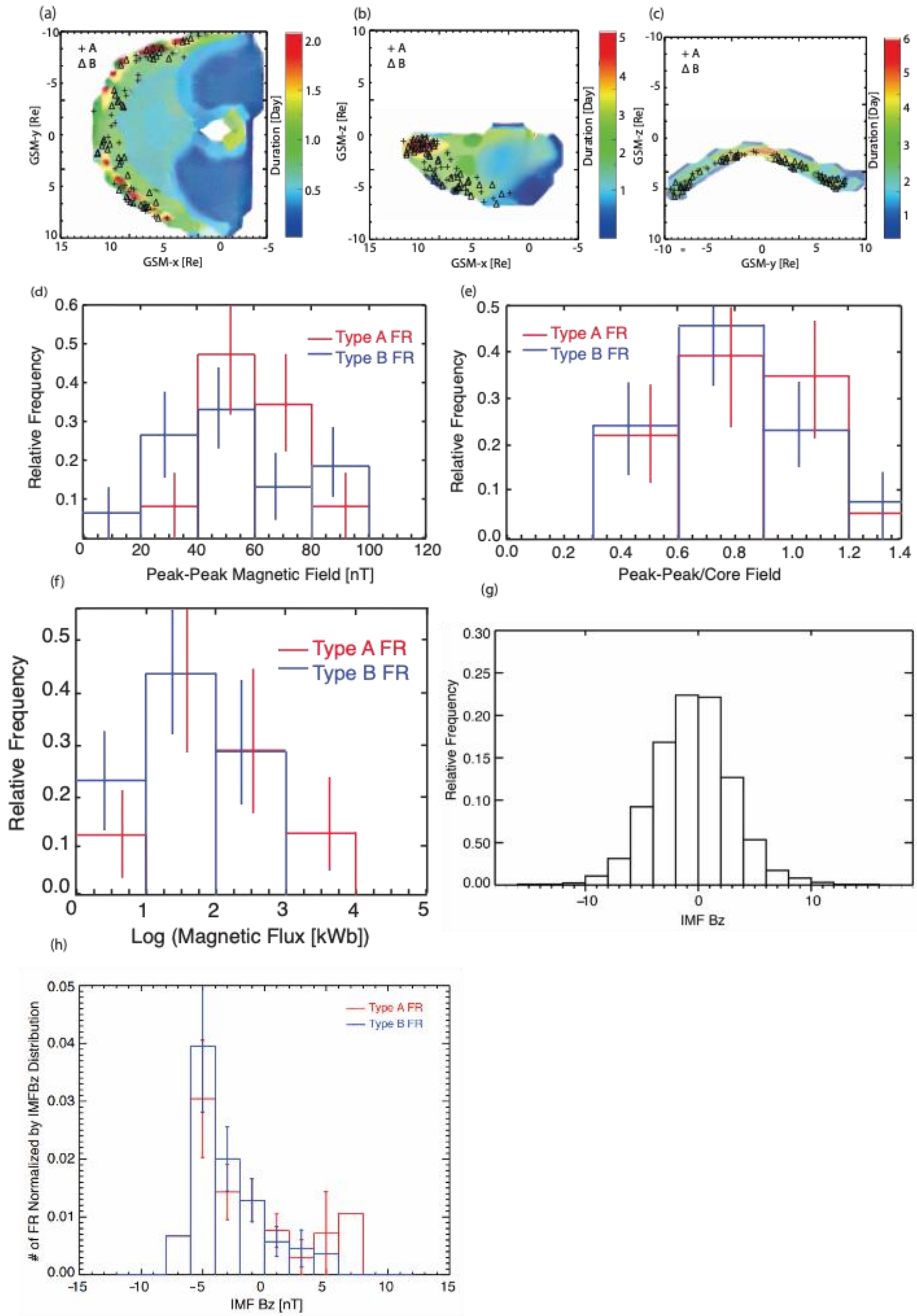
(a)
+ A
Δ B
GSM-y [Re]
GSM-x [Re]
Duration [Day]
(b)
+ A
Δ B
GSM-z [Re]
GSM-x [Re]
Duration [Day]
(c)
+ A
Δ B
GSM-z [Re]
GSM-y [Re]
Duration [Day]
(d)
Type A FR
Type B FR
Relative Frequency
Peak-Peak Magnetic Field [nT]
(e)
Type A FR
Type B FR
Relative Frequency
Peak-Peak/Core Field
(f)
Type A FR
Type B FR
Relative Frequency
Log (Magnetic Flux [kWb])
(g)
Relative Frequency
IMF Bz
(h)
Type A FR
Type B FR
# of FR Normalized by IMFBz Distribution
IMF Bz [nT]

Figure 3. (a)-(c): The location of the crossings of flux tubes by the four MMS spacecraft. The symbols △ and X indicate flux tubes with and without significant fluxes of energetic electrons. These plots show the same spatial distribution for each type of rope. Panel a is the GSM X-Y plane, i.e., the view from above the Earth. Panel b is the Z-X plane, the view from the dusk side. Panel c is the Y-Z plane, i.e., the view from the Sun.; **(d)** Histogram of the occurrence rate of type A and type B ropes as a function of the peak-to-peak field strength. **(e)** Histogram of the occurrence rate of A and B type ropes versus the ratio of the peak-to-peak field divided by the core field strength; **(f):** Histogram of the flux content of the A and B flux ropes, which appear identical; **(g)** The occurrence rate of the north-south component of the interplanetary magnetic field measured by the Wind spacecraft in GSM coordinates in 2nT steps, from -12 to 12 nT; **(h)** The occurrence rate of the two classes of event versus the north-south component of the interplanetary field normalized by the occurrence rate of these north-south fields. The ropes are rare for northward IMF, as measured in the GSM coordinate system. They are also rare to absent for the strongest southward fields, in agreement with the sketch of the field geometry used in Figure 4. (After Zhao, 2019)

We are left with the conclusion that the number of flux ropes empty of magnetospheric energetic electrons exactly matches the number of filled flux ropes. There is only one way that this could occur. The flux rope production process must produce an empty flux tube every time it produces a filled flux tube. This is a very strong constraint on the production mechanism. The sequence of events that makes such paired ropes must occur in common solar wind conditions and must be occurring frequently. In the next section, we discuss how this mechanism can take place, resulting in the production of a flux rope closing in the magnetosphere proper while simultaneously forming a flux rope that has no ends in the magnetosphere. As unlikely as this might seem, it turns out that this production can occur quite naturally.

4 How Pairs of Flux Ropes Can Be Produced

Previous studies (Oieroset et al., 2019; Kacem et al., 2018) have demonstrated the interaction between two converging magnetic flux tubes that come from two different reconnection lines during a period with a moderately southward, or even By-dominant IMF. This configuration is sketched in the left-hand panel of Figure 4a. The connected magnetic field in the south (location 1) and the north (location 2) would each produce two pairs of flux tubes that, on their south/north end, was connected to the south/north polar regions (one to each), and the other pair of flux tubes converge and collide with each other. Then the two tubes would be entangled, as shown in panel (b) of Figure 4. These two entangled ropes would begin to interact and reconnect with their regions of anti-parallel fields, a process termed pileup reconnection. (Pyakurel et al., 2019)

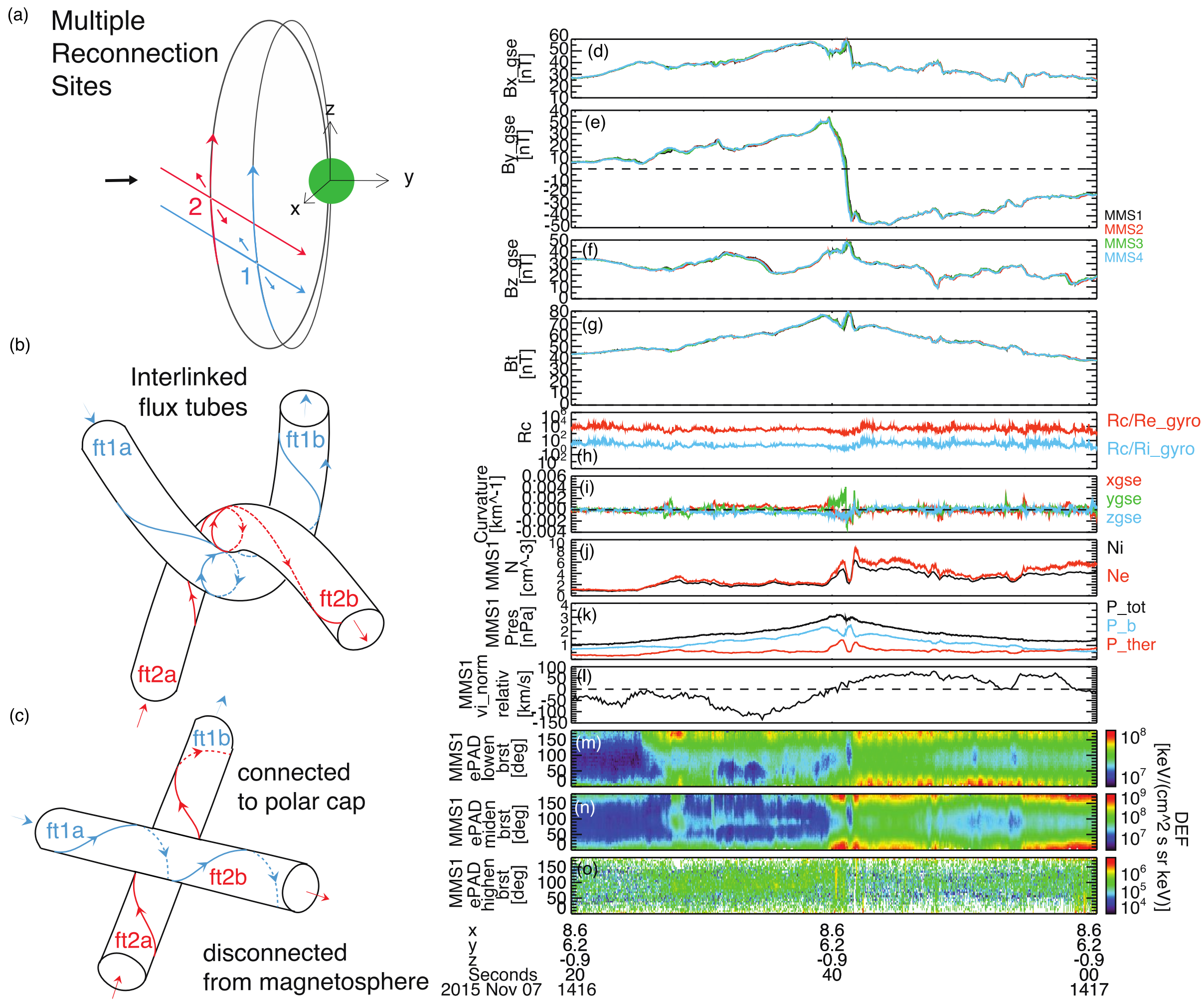

Figure 4. (a), (b) How entangled flux ropes can be produced when the interplanetary magnetic field is southward and oblique to the equator. Reconnection occurs at locations both above and below the equator, and the resulting tubes become entangled, as illustrated on the right. The two flux tubes before reconnection are labeled as FT1a to FT1b, and FT2a to FT2b. These tubes entangle with each other and reconnect at their intersection. **(c)** Eventually, these two tubes develop into two different orthogonal tubes, labeled as FT2a to FT1b, and FT1a to FT2b. The first one connects the two hemispheres (the original legs connected to the north and the south). The second one is not connected to the magnetosphere at all, constructed from the northern section of the rope coming in from the left in panel (b), and the parallel southern sector of the rope going off to the right in panel (b). The geometry of entanglement where the ropes pull against each other is likely to be roughly cylindrical. (d)-(o) an overview plot of a representative event on Nov 7, 2015. (d) – (g) the magnetic field components in GSE coordinates and the field strength observed by four spacecraft; (h),(i) the radius of curvature and curvature vector; (i)-(o) MMS1 observations of the plasma number density; pressure; ion bulk flow velocity perpendicular to the current sheet; and electron pitch angle distribution.

The interface between these two converging tubes undergoes reconnection and annihilates any anti-parallel magnetic field lines at the entanglement, while the parallel segments remained to form two “new” ropes. Before reconnection, field lines are connected to the magnetosphere on one end, and connected to the sheath on the other end. After reconnection, half of the field lines (north pointing as shown in Figure 4c) are connected to the two high-latitude regions in the magnetosphere, and the other half (horizontal as shown in Figure 4c) are completely disconnected from the Earth's magnetic field. On the two sides of the interface, significant field line curvature reverses sign, indicating the opposing tension force on the interface (Figure 4h, i). The entangled parts of the two tubes converge into the reconnecting current sheet, indicated by the relative ion bulk flow velocity in the direction normal to the current sheet. (This is obtained by timing the four spacecraft at 2015-11-07 14:16:41. The normal direction N = [-0.6, -0.07, 0.8] GSE; the current sheet normal speed is 75 km/s). Thus eventually, all the field lines of the initial tubes will reconnect and form a new pair of flux tubes, but now with rotations resulting from the reconnection, and thus identified as FRs. One rope of the pair contains magnetospheric plasmas, and is linked to the polar regions. These are illustrated in Figure 4c. The totally unconnected rope would be free of any energetic particles. The rope connected to the north and south magnetic hemispheres would trap energetic particles. This scenario is in complete accord with the observations. We note that this is the simplest tangled configuration and therefore the more common, and expected, configuration.

In short, the formation of flux transfer events, as described here, does affect both the solar wind connected flux tubes and terrestrial magnetic flux tubes, but not, as originally envisioned by Russell and Elphic (1978, 1979), by convecting flux into the polar cap. Rather, the initial reconnection step that led to the production of the flux tubes, sent the magnetic flux into the two polar caps. This initial poleward transfer of magnetic flux increased the sizes of the two polar caps without entanglement. We now understand that these flux ropes result from interlinked flux tubes generated at two independent reconnection sites: one in each hemisphere, in moderately southward IMF conditions. While initially this leads to a complex magnetic configuration with a tangled magnetic field, magnetic reconnection between the two twisted flux tubes simplifies the magnetic structure, and in the end, produces a simple configuration containing two ropes, one connected to the magnetosphere and one disconnected from it in the nearby solar wind. Rather than making a complicated magnetic field structure even more complex, reconnection returns the system to a simpler, low-energy state. Our observations also reveal that when the IMF is very southward, the tangled fields do not arise, and this process does not occur. When the IMF is horizontal or northward, reconnection appears to be weak, and flux ropes are also not formed. The flux ropes appear principally over an intermediate range of southward-directed interplanetary fields under conditions of moderate and high Mach number solar wind flow.

5 Conclusions

For the most common, moderately southward interplanetary fields, the reconnection of magnetic fields in the magnetosheath with those in the magnetosphere produces both reconnected flux with a simple path to the poles, and magnetic flux that becomes entangled. The stresses produced by entanglement produce magnetic forces that attempt to simplify the magnetic field configuration. The flux tubes that are connected to the magnetosphere recombine to form a closed flux tube twisted by the entanglement and reconnection, and at the same time, produce a second twisted flux tube with an equal amount of flux that is connected to the solar wind. The entanglement created by the finite area of the reconnecting magnetopause surface has resulted in the production of self-balancing flux ropes. The flux transfer to the polar regions/tail has been handled by classical transport processes poleward of the entanglement region.

This lesson from the Earth's magnetopause might have lessons for magnetic reconnections in other venues, such as on the Sun. The Sun produces very large flux ropes that are responsible for coronal mass ejections. There seems to be no consensus on the instability that is responsible for these energetic events, but for the largest events, the rate of occurrence decreases with increasing strength, and their strength, as judged by speed, is grouped in narrow bins (Freed and Russell, 2014). It is possible that the Sun's entanglement also plays a role in creating different types of magnetic ropes, with both open ropes ejected into the solar wind and closed ropes that stay connected to the Sun. Entanglement may be an important step in the evolution of magnetic fields in the cosmos.

Acknowledgments

This research was supported by the NASA Magnetospheric Multiscale Mission, in association with NASA contract NNG04EB99C. The work at UCLA was supported through subcontract 06-001 with the University of New Hampshire. We thank the many individuals who operate the spacecraft and instruments and ensure the data are accurate and are provided to the science team in a timely manner. The geometrical sketches in Figure 4 were inspired and slightly modified from drawings originally produced by K. J. Hwang. No new data were used or created for this research.

References

Burch, J.L., Moore, T.E., Torbert, R.B., Giles, B.L. (2016), Magnetospheric Multiscale Overview and Science Objectives, *Space Sci. Rev.*, 5-21. doi:10.1007/S11214-015-0164-9.

Elphic, R.C. (1990), Observations of flux transfer events: Are FTEs flux ropes, islands, or surfaces waves, in *Physics of Magnetic Flux Ropes: Geophysical Monograph*, Vol. 58, eds. C.T. Russell, E.R. Priest, L.C. Lee, pp. 455-471. doi:10.1029/GM058.

Freed, A.J. & Russell, C.T. (2014), Travel time classification of extreme solar events: Two families and an outlier, *Geophys. Res. Lett.*, 41, 19, doi:10.1002/2014GL061353.

Kacem, I., et al., (2018). Magnetic Reconnection at a Thin Current Sheet Separating Two Interlaced Flux Tubes at the Earth's Magnetopause Journal of Geophysical Research: Space Physics 123(3), 1779-1793. doi:10.1002/2017ja024537

Lee, L.C. & Fu, Z.F. (1985), A theory of magnetic flux transfer at the Earth's magnetopause, *Geophys. Res. Lett.*, 12, 105.

Øieroset, et al. (2019). Reconnection With Magnetic Flux Pileup at the Interface of Converging Jets at the Magnetopause Geophysical Research Letters 46(4), 1937-1946. doi:10.1029/2018gl080994

Pollack, C. et al. (2016), Fast Plasma Investigation for Magnetospheric Multiscale, *Space Sci. Rev.* doi:10.1007/s11214-016-0245-4.

Pyakurel, P., Shay, M., Phan, T., Matthaeus, W., Drake, J., TenBarge, J., Haggerty, C., Klein, K., Cassak, P., Parashar, T., Swisdak, M., Chasapis, A. (2019). Transition from ion-coupled to electron-only reconnection: Basic physics and implications for plasma turbulence Physics of Plasmas 26(8), 082307. https://dx.doi.org/10.1063/1.5090403

Russell, C. T. & Elphic, R. C. (1978), Initial ISEE Magnetometer Results: Magnetopause Observations, *Space Sci. Rev.* 22, 681-715.

Russell, C. T. & Elphic, R.C. (1979), ISEE Observations of Flux Transfer Events at the Dayside Magnetopause, *Geophys. Res. Lett.* 6, 33-36.

Russell, C.T. et al. (2014), The Magnetospheric Multiscale Magnetometers, *Space Sci. Rev.*, 199, 1, 189-256. doi:10.1007/s11214-014-0057-3.

Russell, C., Strangeway, R., Zhao, C., Anderson, B., Baumjohann, W., Bromund, K., Fischer, D., Kepko, L., Le, G., Magnes, W., Nakamura, R., Plaschke, F., Slavin, J., Torbert, R., Moore, T., Paterson, W., Pollock, C., Burch, J. (2017). Structure, force balance, and topology of Earth's magnetopause Science 356(6341), 960-963. doi:10.1126/science.aag3112

Zhao, C. (2019), Statistical Study on Two Types of Flux Transfer Events, Dissertation submitted in partial fulfillment for the degree Doctor of Philosophy in Geophysics and Space Physics, UCLA.